ORIGINAL PAPER

Temperature-treated polyaniline layers as support for Pd catalysts: electrooxidation of glycerol in alkaline medium

Maria Ilieva[1] · **Vessela Tsakova**[1]

Abstract A new approach for obtaining highly dispersed Pd- and Pd/TiO$_2$- electrocatalyst materials is proposed based on the use of polyaniline (PANI) as a sacrificial layer. PANI- or TiO$_2$/PANI-coated electrodes are obtained by electrochemical polymerization of aniline in the absence or presence of TiO$_2$ nanoparticles. Electroless palladium deposition at the expense of PANI oxidation is used to disperse the metal phase. Temperature treatment at 400 °C is further used to decompose the polymer backbone and obtain a highly dispersed catalysts deprived from the intrinsic electroactivity of PANI. The temperature-treated Pd/PANI and Pd/TiO$_2$/PANI composites are studied as catalysts for the electrooxidation of glycerol in alkaline solutions.

Keywords Polyaniline · Palladium · Titanium dioxide · Glycerol

Introduction

In the last two decades, considerable interest was devoted to investigations and development of alternative low-temperature power sources such as direct alcohol fuel cells (DAFCs) converting the free energy of alcohols into electrical energy [1–4]. The choice of the fuel, anode catalyst, and corresponding catalyst support are of utmost importance for the efficiency of DAFCs. Methanol and ethanol have been the subject of numerous studies. However, the strong toxicity and corrosivity of methanol and the high volatility and flammability of ethanol limit their use in DAFCs. Alternatively, the utilization of polyalcohols such as ethylene glycol and glycerol has been proposed in order to overcome these problems. Among these candidates, glycerol has received increasing academic attention as a prospective alcohol fuel due to its extremely low toxicity (even lower than ethanol), weak corrosivity, and high boiling point (290 vs. 78 °C for ethanol and 65 °C for methanol). Furthermore, another important advantage of glycerol is the significant cost decrease as this energy source is obtained as a by-product in the manufacturing of biodiesel [4].

The most important and most expensive component in DAFCs is the electrocatalytic material. Recently, substantial work has been devoted to electrooxidation of alcohols using Pt-based catalysts in alkaline media. In addition to the high costs, many Pt-based catalysts become inhibited in these media because of the tendency of Pt to adsorb carbon monoxide and the following deactivation of the platinum catalyst. Therefore, many efforts were invested in the design of new catalytic materials for DAFC anodes that do not contain Pt [1, 5].

As a substitute to Pt, Pd was demonstrated to be a suitable electrocatalyst for alcohol oxidation [6–13]. The real advantage for Pd-based electrocatalysts originates from the fact that they can be highly active for the oxidation of a large variety of substances in alkaline environment where also non-noble metals are sufficiently stable for electrocatalytic applications [5]. Therefore, the strategy is to combine Pd with other metals, such as Cu, Fe, Co, Sb, Sn, and Pb and obtain bi-metallic catalysts resulting in increased rate of alcohols oxidation [8, 14–16]. A further way is to prepare composite catalysts by coupling Pd with semiconductor oxides and especially TiO$_2$, which was demonstrated to improve the catalytic activity and stability of the Pd catalyst for alcohol electrooxidation [17–23].

✉ Maria Ilieva
milieva@ipc.bas.bg

[1] Institute of Physical Chemistry, Bulgarian Academy of Sciences, 1113 Sofia, Bulgaria

Finally, the third important component of the electrocatalytic system of DAFCs is the material used to support the electrocatalytic species. The main requirements for the supporting materials are high surface area, good electrical and thermal conductivity, low resistance, and high stability [1, 5]. Various forms of carbon (carbon powder, carbon black, carbon nanotubes, carbon nanofibers, etc.) are often used as catalyst support in fuel cells [6–12, 14–18, 21–23]. Conducting polymers (polyaniline, poly(3,4-ethylenedioxithiophene), polypyrrole) are also employed as supports for metals (Pd, Au, Pt, Ni) or metal oxide particles [24–35]. The advantages of conducting polymers as catalyst supports are discussed in terms of high specific surface area, high tolerance to poisoning, and low resistance. In almost all studies involving conducting polymers as supports they are used for their high electrical conductivity. The intrinsic redox electroactivity is in the origin of polymer-based electrocatalytic response for some electrochemical reactions.

Although polyaniline (PANI) is often studied as support for metal or metal oxide particles [27, 29, 33, 35] it has a basic limitation concerning the high acidity of the electrochemical solution that should be used for electrocatalytic purposes. In neutral and alkaline solutions, PANI becomes deprotonated and loses its high electrical conductivity and thus also the electrical contact between deposited metal particles and underlying electrode. For that reason, almost all (except, e.g., [28]) investigations on PANI-based materials avoid to use alkaline media.

In previous investigations, we have used polyaniline as support for TiO_2 nanoparticles (NPs) [36, 37] with the intention to disperse the semiconducting photocatalytic NPs in the volume of the conducting polymer matrix. Furthermore, we suggested using PANI only as a sacrificial layer necessary for the initial immobilization of the TiO_2 NPs [37]. After electrochemical polymerization of aniline in the presence of the metal oxide NPs, the resulting composite layers were annealed at high temperature in order to decompose the PANI structure. Thus, PANI became deprived from its intrinsic redox electroactivity but nevertheless highly dispersed photoelectrocatalytic materials were obtained.

In this investigation, we suggest a similar approach for producing supported highly dispersed Pd-based electrocatalysts. Electrochemically obtained PANI layers (with and without TiO_2 NPs) are used for electroless deposition of Pd. The electroless metal deposition process occurs at the expense of the spontaneous oxidation of initially reduced PANI layers [25, 27, 29]. After obtaining the Pd-modified PANI- or TiO_2/PANI-coated electrodes they are annealed in order to decompose the PANI structure. The Pd-based catalysts obtained after temperature treatment are investigated for electrooxidation of glycerol.

Experimental

All experiments were carried out in three electrode cells at room temperature using platinum plates as counter electrodes and saturated mercury/mercury sulfate/0.5 M K_2SO_4 reference electrodes (MSE). All potentials in the text are referred to MSE (E_{MSE}=0.66 V vs. standard hydrogen electrode). The working electrode consisted of a spectroscopically pure graphite rod with a diameter 0.2 cm (S+E Carbopur, Schunk & Ebe GMBH, Giessen) put in a mechanical pencil (KOH-I-NOOR Versatil 5201). The active surface area was fixed at 0.23 cm^2 by using Teflon band to wrap the upper part of the graphite rod. After completing the experimental series, the used part of the graphite rod was cut off and a fresh surface area was used for the next experimental sequence.

The electrolytic solutions were prepared with ultrapure water obtained from a Millipore Synergy™ Ultrapure Water Purification System and were de-aerated with argon for at least 30 min before the onset of the electrochemical measurements. The electrochemical measurements were carried out with a computerized potentiostat/ galvanostat Autolab PGSTAT-12, Ecochemie, (The Netherlands).

Each experiment consisted of several consecutive steps performed in six electrochemical cells:

1. Electrochemical polymerization of aniline in the absence or presence of TiO_2 nanoparticles by cyclic voltammetry between −0.66 and +0.345 V vs. MSE at 0.1 V s^{-1} in an aqueous solution of 0.1 M aniline and 0.5 M H_2SO_4. A supplement of 20 g l^{-1} of TiO_2 nanoparticles (NPs) (P25 powder of Degussa) was used for the preparation of the TiO_2/PANI composite layers [36]. In this case, constant magnetic stirring was used to promote the uptake of TiO_2 particles during the electrodeposition process.

2. Characterization of the redox activity of the synthesized PANI- or TiO_2/PANI-coated electrodes in acid supporting electrolyte (0.5 M H_2SO_4) by cyclic voltammetry between −0.66 and +0.32 V at a sweep rate of 0.1 V s^{-1}. The redox charge obtained by integrating the voltammetric curve was used as an indirect measure of the thickness of the polymer layers. In the same electrolyte, the polymer layers were electrochemically reduced by keeping the electrodes at constant potential E=−0.66 V vs MSE for 900 s. Thus, the PANI layers were converted from emeraldine in leucoemeraldine oxidation state.

3. Electroless deposition of palladium NPs was carried out by dipping the pre-reduced PANI or TiO_2/PANI layers in an aqueous solution of 0.002 M $PdSO_4$ and 0.5 M H_2SO_4.

4. Temperature treatment of the obtained PANI or TiO_2/PANI-coated electrodes in order to deactivate the polymer structure. This step was carried out in a furnace in ambient atmosphere at 400 ° for 1.30 h. This temperature was chosen based on studies showing that up to 400 °C PANI

loses about 20 % from its mass and specific chemical changes take place without formation of graphitic structures [38–42]. The temperature-treated Pd-modified electrodes are further denoted as *t*-Pd/PANI or *t*-Pd/TiO$_2$/PANI.

5. Characterization of the redox activity of the Pd-modified PANI or TiO$_2$/PANI electrodes in acid supporting electrolyte (0.5 M H$_2$SO$_4$) by cyclic voltammetry between −0.66 and +0.72 V at a sweep rate of 0.02 V s^{-1} in order to reveal the existence and electroactivity of the deposited palladium NPs.
6. Reference measurements in alkaline supporting electrolyte (0.5 M KOH), in the absence of glycerol, by cyclic voltammetry between −1.0 and −0.1 V vs. MSE at 0.02 V s^{-1}.
7. Electrooxidation of glycerol in the presence of 0.1 M glycerol in 0.5 M KOH by cyclic voltammetry between −1.0 and −0.1 V vs. MSE at 0.02 V s^{-1} for assessing the electrocatalytic activity of the Pd/PANI-coated electrodes.
8. Repeated voltammetric measurements in 0.5 M KOH, in the absence of glycerol, in order to compare the state of the *t*-Pd/PANI and *t*-Pd/TiO$_2$/PANI layers before and after exposure to glycerol.
9. Anodic dissolution of Pd in 1.15 M HCl aqueous solution by sweeping the potential from −0.13 to +0.32 V with a scan rate of 0.005 V s^{-1}. This final step of each experimental sequence provided the possibility to determine the amount of metal that was plated in the course of the electroless deposition and involved in the electrocatalytic measurements.

Scanning electron microscopy (SEM) imaging and energy dispersive x-ray (EDX) analysis was accomplished by means of a SM 6380 (JEOL) apparatus equipped with an INCA Oxford 7582 system.

Results and discussion

Formation and characterization of Pd/PANI and Pd/TiO$_2$/PANI layers

The investigations of the electrochemical synthesis of PANI on graphite electrodes have shown that under potentiodynamic conditions, the polymerization occurs in a similar way both in the absence and the presence of TiO$_2$ NPs. It was found that the deposited polymer layers have identical redox charge for roughly the same number of voltammetric scans (Fig. 1). The availability of TiO$_2$ in the composite layers was registered by means of EDX analysis showing large amounts of TiO$_2$ evenly distributed on the electrode surface.

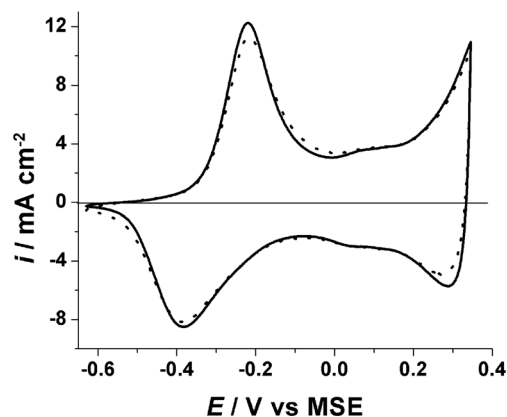The electrochemical synthesis of the PANI- or TiO$_2$/PANI-coated electrodes was followed by electrochemical reduction

Fig. 1 Cyclic voltammograms recorded at the modified electrodes after potentiodynamic polymerization of PANI (*solid line*) and TiO$_2$/PANI (*dashed line*), q_{redox}(PANI)=36.8 mC cm^{-2} for 97 scans, q_{redox}(TiO$_2$-PANI)=36.7 mC cm^{-2} for 98 scans, v=0.1 V s^{-1}

of the conducting polymer layers and electroless deposition of Pd. The equilibrium potential of Pd/Pd^{2+} ($E^0_{Pd^{2+}/Pd}$=0.175 V vs MSE) is positive enough with respect to the reduction potential used for conditioning the PANI layers. The spontaneous process of PANI oxidation at the expense of Pd^{2+} ions reduction was followed by monitoring the open circuit potential (OCP) of the polymer-coated electrode. Typical OCP transient registered when immersing reduced PANI-coated electrode in the Pd-ions containing solution shows a steep potential increase in the first 400 s (Fig. 2, inset). In this time span, the OCP of the pre-reduced PANI-coated electrode immersed in a blank solution (without metal ions) shows a sluggish change in potentials up to −0.45 V [29, 43]. On the other hand, the potential interval where the electroless deposition occurs is far from potentials where hydrogen sorption phenomena on Pd could be observed. Thus, the OCPs shown in Fig. 2 reflect only the oxidation of the PANI layer occurring at the expense of metal ions reduction. In our further experiments on Pd electroless deposition, the process was interrupted once the
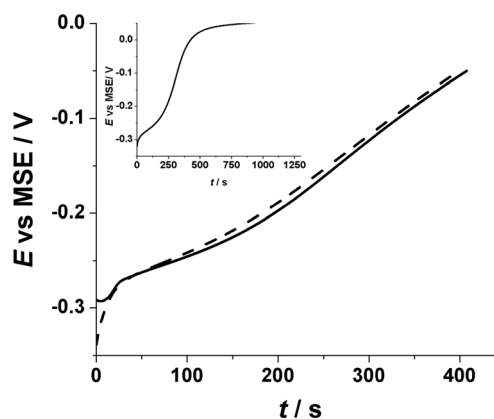

Fig. 2 Open circuit potential transients measured in 0.002 M PdSO$_4$ and 0.5 M H$_2$SO$_4$ for PANI-(*solid line*) and TiO$_2$/PANI-(*dashed line*) modified electrodes. *Inset* OCP measured at PANI-modified electrode in a longer time scale

Fig. 3 Voltammetric curves
measured in 0.5 M $H_2SO_4^+$, **a**
Before annealing at PANI (*solid
line*) and Pd/ PANI (*dotted line*)
modified electrodes. **b** After
annealing at *t*-Pd/PANI (*solid
line*) and *t*-Pd/TiO$_2$/PANI (*dashed
line*) modified electrodes,
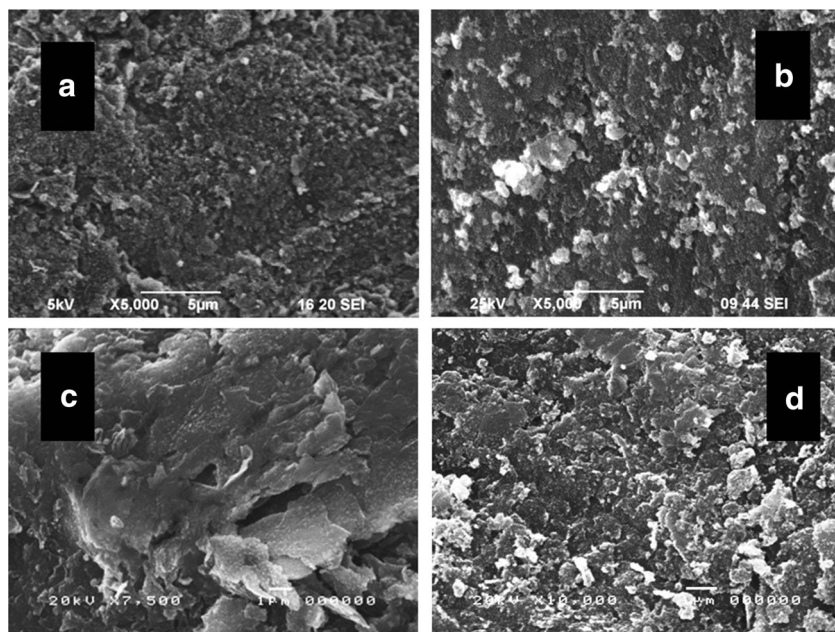$v=0.02$ V s^{-1}
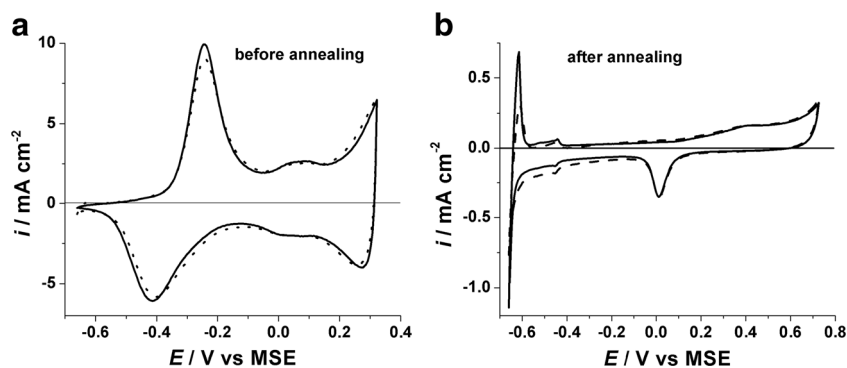
potential of −0.05 V was reached for both PANI- and TiO$_2$/
PANI specimens.

Figure 3a shows cyclic voltammograms of a PANI-coated
electrode registered in acidic medium before and after electro-
less deposition of Pd. Due to the large intrinsic oxidative/
reductive currents of PANI, the typical Pd-related hydrogen
adsorption/desorption electrochemical signals can be hardly
detected in this measurement. After thermal treatment, the
electrochemical behavior of the *t*-Pd/PANI and *t*-Pd/TiO$_2$/
PANI-modified electrodes was tested again in acidic solution
(Fig. 3b). The voltammograms show already clear hydrogen
adsorption/desorption peaks in the potential range −0.4 to
−0.7 V and peaks associated with the formation/reduction of
PdO (−0.1 to 0.8 V) at the surface of the palladium species
immobilized on the annealed electrode. The typical fingerprint
of the PANI electroactivity is not available any more indicat-
ing to the thermally induced decomposition of the PANI-
conjugated backbone. The electrochemically active surface
area of Pd was evaluated by integrating the charge of the
PdO reduction peak. Taking 424 μC cm^{-2} as reference value

for the PdO reduction charge, the active surface area of the
deposited Pd was found to be 3.1 cm^2.

The surface of the *t*-Pd/PANI and *t*-Pd/TiO$_2$/PANI electrodes
was studied by SEM (Fig. 4) and EDX analysis. The SEM
images of the *t*-Pd/TiO$_2$/PANI specimen (Fig. 4b, d) show
rougher surface structures in comparison to the *t*-Pd/PANI spec-
imen. Our former studies on the electrochemical polymerization
of aniline in the presence of TiO$_2$ NPs [36] have shown that the
rough surface morphology is available already after the forma-
tion of the TiO$_2$/PANI composite layer. Due to their small size,
the individual Pd particles could not be easily detected. The fine
sand-like features observed at the flat areas of the specimen in
Fig.4c give evidence for the presence of a high number of evenly
distributed Pd NPs. SEM images taken at larger magnification
(not shown because of lack of sharpness) provided the possibil-
ity to estimate the size of the Pd particles to vary between 40 and
80 nm. Direct evidence for the presence of Pd on *t*-Pd/PANI and
t-Pd/TiO$_2$/PANI layers was obtained by EDX analysis. Further-
more, after completing the electrocatalytic experiments, the de-
posited Pd was electrochemically dissolved by a voltammetric

Fig. 4 SEM images of *t*-Pd/PANI
(**a**, **c**) and *t*-Pd/TiO$_2$/PANI (**b**, **d**)
surfaces at different
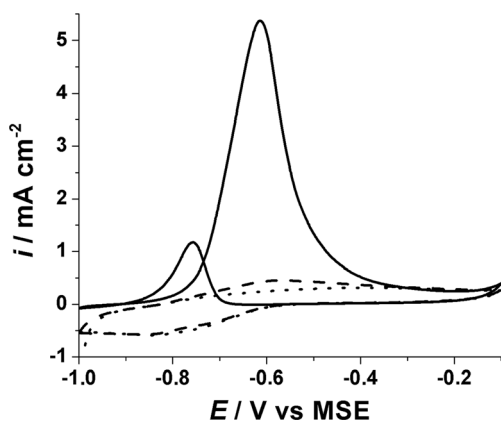magnifications

Fig. 5 Cyclic voltammetric curves measured in 0.5 M KOH and 0.1 M glycerol at Pd/TiO$_2$/PANI-modified electrode before (*dashed line*) and after (*solid line*) annealing; the *dotted line* is measured before annealing in KOH alone. v=0.02 V s^{-1}

scan carried out in 1.15 M HCl. The amount of dissolved Pd, calculated by means of the oxidation charge of the dissolution peak, was found to be practically the same (21 μg cm^{-2}) for *t*-Pd/PANI and *t*-Pd/TiO$_2$/PANI-modified electrodes with equal redox charge (37 mC cm^{-2}) of the PANI layers. Assuming a hemispherical shape of the Pd particles and taking the data for the mass of deposited Pd and thus its volume and the electroactive surface area estimated above it was possible to calculate the mean size of the Pd particles. It was found to be 35 nm in diameter which is somewhat smaller than the size obtained by direct microscopic observation. This discrepancy might be due to the fact that the SEM micrographs at high magnification are taken at the limits of the technical possibilities of our SEM device which means that smaller particles could not be technically detected. The number of particles obtained through the electroless deposition was estimated by using the data for the mass of the Pd particles and the estimated mean diameter and was found to be 1.8×10^{11} cm^{-2}.

Electrocatalytic investigations

The modified electrodes were further studied for their response in alkaline solutions in the absence and the presence

of 0.1 M glycerol. Voltammetric studies of Pd/TiO$_2$/PANI-modified electrodes before temperature treatment are shown in Fig. 5 (dotted and dashed lines). The addition of glycerol has a slight effect on the voltammetric response showing a weak oxidation peak centered at about −0.58 V. Bearing in mind that in alkaline solutions, PANI suffers a strong decrease in electrical conductivity, this result should mean that before annealing, most of the Pd particles have no direct contact with the underlying graphite substrate and are not operative for the electrocatalytic reaction. The observed slight electrocatalytic activity contradicts the observations of Hatchett et al. [28] which report on strong electrocatalytic activity of Pd/PANI-modified electrodes for methanol oxidation in alkaline solutions. It was suggested that Pd acts as a solid state dopant that may delocalize the charge on the polymer backbone to maintain conductivity in the absence of proton doping. We did not observe such an effect but it is worth noting that the Pd NPs were deposited in very different ways. Electrochemical reduction under potentiodynamic cycling in a solution of anionic metal complexes of Pd with no acid was carried out in [28] whereas electroless reduction of Pd^{2+} cations on pre-reduced PANI in acidic solution was used in the present case.

The voltammogram recorded on the same modified electrode after annealing is shown in Fig. 5 (solid line). In the presence of glycerol, a strong symmetric anodic oxidation peak is observed in the forward scan followed by a much weaker oxidation peak in the backward scan. The latter is usually attributed to the removal of the incompletely oxidized carbonaceous species obtained in the course of glycerol oxidation.

Further measurements were made in order to compare the electrocatalytic behavior of *t*-Pd/PANI- and *t*-Pd/TiO$_2$/PANI-modified electrodes. Twenty consecutive voltammetric scans were measured in the presence of glycerol for both types of electrodes (Fig. 6). For both specimens, a gradual conditioning of the electrodes with respect to peak maxima and peak position was observed. The data for the forward peak currents and the forward to backward peak ratio in dependence of the scan number are summarized in Fig. 7. The absolute peak values are comparable for both types of modified electrodes

Fig. 6 Twenty consecutive cyclic voltammetric curves measured in 0.1 M glycerol and 0.5 M KOH at **a** *t*-Pd/PANI and **b** *t*-Pd/TiO$_2$/PANI-modified electrodes, q_{redox}(PANI)=36.7 mC cm^{-2}, v=0.02 V s^{-1}
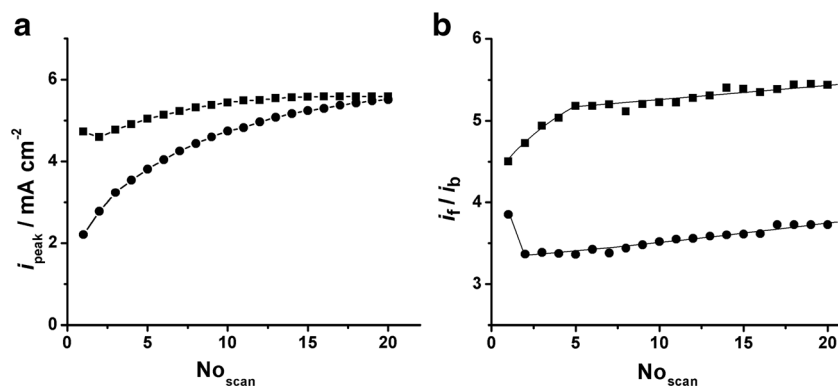
as should be expected based on the equal amount of the dispersed catalytic metal.

The data for the forward to backward current peak ratio, i_f/i_b, (Fig. 7b) are frequently used to evaluate the tolerance of the catalyst to the accumulation of carbonaceous species on the Pd surface. A higher i_f/i_b ratio is obtained for the *t*-Pd/TiO$_2$/PANI catalyst indicates a higher efficiency of this catalyst. This means that the TiO$_2$ particles support the oxidation of carbonaceous residues adsorbed on Pd and prevent their excessive accumulation on the catalytic surface. Studies on oxide-promoted Pd/C catalysts have shown that the content of the oxide plays a significant role for the electrocatalytic performance of composite Pd-based catalysts [17, 23]. Further optimization of the Pd/TiO$_2$/PANI material in terms of Pd toTO$_2$ content is necessary in order to find the best performing conditions.

Conclusions

In the present investigation, we suggest a new approach for obtaining highly dispersed Pd NP-based catalysts suitable for applications in alkaline solutions. Polyaniline is used only as a sacrificial layer necessary to disperse the metal phase through electroless metal ions reduction occurring at the expense of the polymer oxidation. PANI is further decomposed by means of temperature treatment that results in a Pd- or Pd/TiO$_2$-modified electrodes without intrinsic PANI-based electroactivity. Under the conditions of our experiments, Pd NPs with an average size of about 40 nm and surface density of about 1.8×10^{11} cm^{-2} were obtained. The catalyst loading amounted to 20 µg/cm^2 and thus a value of 300 mA/(cm^{-2} mg) was obtained for the mass electroactivity of the catalyst. In comparison to existing data for glycerol oxidation on Pd-based catalysts [13, 15, 44] this is a competitive value obtained at a very low Pd consumption. The high i_f/i_b ratio of the Pd catalysts used in this study, which in all cases exceeds 3.3, indicates to an effective electrocatalytic process supported very probably by surface species resulting from annealing of the PANI structure. In fact, the temperature treatment at a mild

temperature (up to 400 °C) results in cross-linking of the PANI chains and formation of phenazine heterocycles [38, 41] and thus in a new surface chemical modification of the electrode.

The attempt to combine Pd and TiO$_2$ by the approach developed in this study resulted in higher i_f/i_b ratios amounting to 5.5. This points to the expected advantageous role of the TiO$_2$ NPs for the oxidation of residual carbonaceous species. By further optimization of the Pd/TiO$_2$ content, possibly higher electroactivity of the Pd/TiO$_2$ catalyst could be achieved. It is also worth emphasizing that graphite electrodes without special surface pre-treatment were used in the present study.

Finally, it is worth stressing that the developed approach is most flexible and allows modifying the amount and distribution of the metallic phase by employing PANI layers with different redox charges. By varying the metal precursor, i.e., metal cations or metal anion complexes a further variation in the type of the metal deposit could be achieved. Depending on the temperature used for annealing of the PANI layers, various surface species are obtained and a different impact on the studied electrocatalytic reactions could be expected. Thus, the present study is only a first step on the way of obtaining metal-based catalysts combining the opportunity to disperse finely the metal phase due to the intrinsic redox properties of conducting polymer layers and the possibility to eliminate the polymer-based electroactivity and obtain a new chemically modified surface.

References

1. Antolini E, Gonzalez ER (2010) Alkaline direct alcohol fuel cells. J Power Sources 195:3431–3450
2. Lavacchi A, Miller H, Vizza F (2013) Nanotechnology in electrocatalysis for energy. Springer, New York, **331 p**. ISBN 978-1-4899-8059-5

3. Braunchweig B, Hibbitts D, Neurock M, Wieckowski A (2013) Electrocatalysis: a direct alcohol fuel cell and surface science perspective. Catal Today 202:197–209

4. Quispe CAG, Coronado CJR, Carvalho JA Jr (2013) Glycerol: production, consumption, prices, characterization and new trends in combustion. Renew Sust Energ Rev 27:475–493

5. Bianchini C, Shen PK (2009) Palladium-based electrocatalysts for alcohol oxidation in half cells and in direct alcohol fuel cells. Chem Rev 109:4183–4206

6. Wang Z, Hu F, Shen PK (2006) Carbonized porous anodic alumina as electrocatalyst support for alcohol oxidation. Electrochem Commun 8:1764–1768

7. Bambagioni V, Biamchini C, Marchionni A, Filippi J, Vizza F, Teddy J, Serp P, Zhiani M (2009) Pd and Pt-Ru anode electrocatalysts supported on multi-walled carbon nanotubes and their use in passive and active direct alcohol fuel cells with an anion-exchange membrane (alcohol=methanol, ethanol, glycerol). J Power Sources 190:241–251

8. Simoes M, Baranton S, Contanceau C (2010) Electrooxidation of glycerol at Pd-based nano-catalysts for an application in alkaline fuel cells for chemicals and energy cogeneration. Appl Catal B Environ 93:354–362

9. Habibi E, Razmi H (2012) Glycerol electrooxidation on Pd, Pt and Au nanoparticles supported on carbon ceramic electrode in alkaline media. Int J Hydrogen Energy 37:16800–16809

10. Machado BF, Marchionni A, Bacsa RR, Bellini M, Beausoleil J, Oberhauser W, Vizza F, Serp P (2013) Synergistic effect between few layer graphene and carbon nanotube supports for palladium catalyzing electrochemical oxidation of alcohols. J Energy Chem 22:296–304

11. Dector A, Cuevas-Mun FM, Guerra-Balcazar M, Godinez LA, Ledesma-Garcia J, Arriaga LG (2013) Glycerol oxidation in a microfluidic fuel cell using Pd/C and Pd/MWCNT anodes electrodes. Int J Hydrogen Energy 38:12617–12622

12. Li SS, Hu YY, Feng JJ, Lv ZY, Chen JR, Wang AJ (2014) Rapid room-temperature synthesis of Pd nanodendrites on reduced graphene oxide for catalytic oxidation of ethylene glycol and glycerol. Int J Hydrogen Energy 39:3730–3738

13. Rezaei B, Havakeshian E, Ensafi AA (2014) Fabrication of porous Pd film on nanoporous stainless steel using galvanic replacement as a novel electrocatalyst/electrode design for glycerol oxidation. Electrochim Acta 136:89–96

14. Maya-Cornejo J, Arjona N, Guerra-Balcázar M, Álvarez-Contreras L, Ledesma-García J, Arriaga LG (2014) Synthesis of Pd-Cu bimetallic electrocatalyst for ethylene glycol and glycerol oxidations in alkaline media. Proc Chem 12:19–26

15. Fashedemi OO, Ozoemena KI (2014) Comparative electrocatalytic oxidation of ethanol, ethylene glycol and glycerol in alkaline medium at Pd-decorated FeCo@Fe/C core-shell nanocatalyst. Electrochim Acta 128:279–286

16. Sadiki TA, Vo P, Hu S, Copenhaver TS, Scudiero L, Ha S, Haan JL (2014) Increased electrochemical oxidation rate of alcohols in alkaline media on palladium surfaces electrochemically modified by antimony, lead, and tin. Electrochim Acta 13:302–307

17. Xu C, Tian Z, Shen P, Jiang SP (2008) Oxide (CeO_2, NiO, Co_3O_4 and Mn_3O_4)-promoted Pd/C electrcatalysts for alcohol electrooxidation in alkaline media. Electrochim Acta 53:2610–2618

18. Hu F, Ding F, Song S, Shen P (2006) Pd electrocatalyst supported on carbonized TiO_2 nanotubes for ethanol oxidation. J Power Sources 163:415–419

19. Su L, Jia W, Schempf A, Lei Y (2009) Palladium/titanium dioxide nanofibers for glycerol electrooxidation in alkaline medium. Electrochem Commun 11:2199–2202

20. Xu W, Zhu S, Li Z, Cui Z, Yang X (2013) Synthesis and catalytic properties of Pd nanoparticles loaded nanoporous TiO_2 material. Electrochim Acta 114:35–41

21. Estudillo-Wong LA, Vargas-Gomez AM, Arce-Estrada EM, Manzo-Robledo A (2013) TiO_2/C composite as a support for Pd-nanoparticles toward the electrocatalytic oxidation of methanol in alkaline media. Electrochim Acta 112:164–170

22. Liang R, Hu A, Persic J, Zhou N (2013) Palladium nanoparticles loaded on carbon modified TiO_2 nanobelts for enhanced methanol electrooxidation. Nano Micro Lett 5:202–212

23. Maheswari S, Sridhar P, Pitchumani S (2013) Pd-TiO_2/C as a methanol tolerant catalysts for oxygen reduction reaction in alkaline medium. Electrochem Commun 26:97–100

24. Venancio EC, Napporn WT, Motheo AJ (2002) Electro-oxidation of glycerol on platinum dispersed in polyaniline matrices. Electrochim Acta 47:1495–1501

25. Tsakova V (2008) How to affect number, size, and location of metal particles deposited in conducting polymer layers. J Solid State Electrochem 12:1421–1434

26. Antolini E, Gonzalez ER (2009) Polymer supports for low-temperature fuel cell catalysts. Appl Catal A 365:1–19

27. Tsakova V (2010) Metal-based composite of conducting polymers. In: Eftekhari A (ed) Nanostructured conductive polymers, Wiley. ISBN 978-0-470-74585 289-340

28. Hatchett DW, Millick NM, Kinyanjui JM, Pookpanratana S, Bar M, Hofmann T, Heske C (2011) The electrochemical reduction of $PdCl_4^{2-}$ and $PdCl_6^{2-}$ in polyaniline: influence of Pd deposit morphology on methanol oxidation in alkaline solution. Electrochim Acta 56:6060–6070

29. Lyutov V, Tsakova V (2011) Palladium-modified polysulfonic acid-doped polyaniline layers for hydrazine oxidation in neutral solutions. J Electroanal Chem 661:186–191

30. Ciric-Marjanovic G (2013) Recent advances in polyaniline composites with metals, metaloids and nonmetals. Synth Met 170:31–56

31. Pandey RK, Lakshminarayanan V (2012) Ethanol electrocatalysis on gold and conducting polymer nanocomposites: a study of the kinetic parameters. Appl Catal B Environ 125:271–281

32. Dash S, Munichandraiah N (2012) Electrocatalytic oxidation of 1, 2-propanediol on electrodeposited Pd–poly(3,4-ethylenedioxythiophene) nanodendrite films in alkaline medium. Electrochim Acta 80:68–76

33. Lina H, Yang J, Liu J, Huang Y, Xiao J, Zhang X (2013) Properties of Pd nanoparticles-embedded polyaniline multilayer film and its electrocatalytic activity for hydrazine oxidation. Electrochim Acta 90:382–392

34. Jiang F, Yao Z, Yue R, Xu J, Du Y, Yang P, Wang C (2013) Electrocatalytic activity of Pd nanoparticles supported on poly(3, 4-ethylenedioxythiophene)-graphene hybrid for ethanol electrooxidation. J Solid State Electrochem 17:1039–1047

35. Yan R, Jin B (2014) Preparation and electrochemical performance of polyaniline/Pt microelectrodes. Electrochim Acta 115:449–453

36. Ilieva M, Ivanov S, Tsakova V (2008) Electrochemical synthesis and characterization of TiO_2-polyaniline composite layers. J Appl Electrochem 38:63–69

37. Ilieva M, Tsakova V (2012) TiO_2/WO_3 hybrid structures produced through a sacrificial polymer layer technique for photo- and photoelectrooxidation under ultraviolet and visible light illumination. J Appl Electrochem 42:121–129

38. Trchova M, Matejka P, Brodinova J, Kalnedova A, Prokes J, Stejskal J (2006) Structural and conductivity changes during the pyrolysis of polyaniline base. Polym Degrad Stab 91:114–121

39. Perreira de Silva JE, de Faria DLA, Cordoba de Torresi SI, Temperini MLA (2000) Influence of thermal treatment on doped polyaniline studied by resonance Raman spectroscopy. Macromolecules 33:3077–3083

40. Bhandra S, Khastgir D (2008) Extrinsic and intrinsic structural change during heat treatment of polyaniline. Polym Degrad Stab 93:1094–1099

41. Nand AN, Ray S, Gizdavic- Nikolaidis M, Travas-Sejdic J, Kilmartin PA (2011) The effects of thermal treatment on the anti-oxidant activity of polyaniline. Polym Degrad Stab 96:2159–2166

42. Nishara Begum A, Dhachanamoorthi N, Raja Saravanan ME, Jayamurugan P, Manoharan D, Ponnuswamy V (2013) Influence of annealing effects on polyaniline for good microstructural modification. Optik 124:238–242

43. Ivanov S, Tsakova V (2005) Electroless versus electrodriven deposition of silver crystals in polyaniline: role of silver anion complexes. Electrochim Acta 50:5616–5623

44. Serov A, Martinez U, Atanassov P (2013) Novel Pd-In catalysts for alcohol electrooxidation in alkaline media. Electrochem Commun 34:185–188